



6-2017

Empirical validation of a spined sagittal-plane quadrupedal model

Jeff Duperret

University of Pennsylvania, jdup@seas.upenn.edu

Daniel E. Koditschek

University of Pennsylvania, kod@seas.upenn.edu

Follow this and additional works at: https://repository.upenn.edu/ese_papers



Part of the [Controls and Control Theory Commons](#), and the [Robotics Commons](#)

Recommended Citation

Jeff Duperret and Daniel E. Koditschek, "Empirical validation of a spined sagittal-plane quadrupedal model", *IEEE International Conference on Robotics and Automation* . June 2017.

This paper is posted at ScholarlyCommons. https://repository.upenn.edu/ese_papers/786

For more information, please contact repository@pobox.upenn.edu.

Empirical validation of a spined sagittal-plane quadrupedal model

Abstract

We document empirically stable bounding using an actively powered spine on the Inu quadrupedal robot, and propose a reduced-order model to capture the dynamics associated with this additional, actuated spine degree of freedom. This model is sufficiently accurate as to roughly describe the robots mass center trajectory during a bounding limit cycle, thus making it a potential option for low dimensional representations of spine actuation in steady-state legged locomotion.

Disciplines

Controls and Control Theory | Electrical and Computer Engineering | Engineering | Robotics

Empirical validation of a spined sagittal-plane quadrupedal model

Jeffrey Duperret and Daniel E. Koditschek

Abstract—We document empirically stable bounding using an actively powered spine on the Inu quadrupedal robot, and propose a reduced-order model to capture the dynamics associated with this additional, actuated spine degree of freedom. This model is sufficiently accurate as to roughly describe the robots mass center trajectory during a bounding limit cycle, thus making it a potential option for low dimensional representations of spine actuation in steady-state legged locomotion.

I. INTRODUCTION

Legged robots capable of rapid, efficient performance in any way comparable to that of their biological counterparts over uneven, broken, unstable terrain inaccessible to wheeled or tracked vehicles would radically benefit applications ranging from search-and-rescue operations to the transportation of goods and services. Yet decades of work on legged platforms [1] has thus far largely yielded designs that attach legs to rigid-bodies, despite the abundance of morphological diversity in biology such as tails and spines that contribute to locomotion prowess. In particular, locomotion using a flexible trunk or spine is poorly understood in robotics despite its fundamental role in biological legged locomotion [2]. Throughout this paper we use “spine actuation” and “core actuation” to refer to actuated degrees of freedom proximal to rather than distal from the mass center. A better understanding of robotic core actuation – particularly for quadrupedal running where core actuation is commonly used in biology – is needed to quantify its advantages and disadvantages for designers.

The biological literature on core actuation offers several careful studies regarding its low-level mechanics [3], [4], [5] and its proposed role as a mechanical energy storage in gaits [6]. To the best of the authors’ knowledge, however, there is a lack of work concerning biological templates [7] of core actuation. Such theory – or even adequate reduced-order models – would greatly benefit legged robotics, much as the simple but effective models arising from recent research into tailed animal morphologies [8] has impacted the field [9].

An array of simulation studies of steady-state robotic quadrupedal running utilizing core actuation and compliance has generated a class of reduced-order models that suggest speed and stability benefits [10], [11], [12], [13], yet verifying these models on power-autonomous physical machines remains open. Progress towards this goal was made by the servo-driven Bobcat robot utilizing off-board power [14]. The design of the power-autonomous MIT Cheetah utilizing core actuation is presented in [15] but only simulation data

appears to be given. Other spined platforms exist such as the Canid robot but have only been documented executing non-steady-state tasks [16], [17], [18].

This paper provides empirical documentation¹ of steady-state spined-quadrupedal bounding² at modest speeds utilizing core actuation on a power-autonomous physical machine (the first such documentation in the literature to our knowledge). We compare this steady-state behavior to a simple reduced-order model of a spined quadruped and show rough correspondence between the two, concluding that the proposed simplified model is sufficiently descriptive to exhibit realistic bounding limit cycles utilizing core actuation and is thus of interest for robotic and biological applications, motivating a more formal data-driven analysis for future work along the lines of [20], [21].

II. SAGITTAL-PLANE REDUCED-ORDER MODEL OF SPINED QUADRUPED

Following [11], [12], [13], [15], [18], we propose a reduced-order sagittal-plane spined quadrupedal model consisting of two bipedal body segments connected by a massless pin joint³ as shown in Figure 1. We take the state of the model to be given by $\mathbf{q} = (x, z, \phi, \psi)^T \in \mathcal{Q} = \mathbb{R}^2 \times \mathbb{T}^2$ and its time derivative, where x and z respectively denote the horizontal and vertical displacement of the mass center from the origin, ϕ denotes the body pitch, and ψ denotes the angle of the spine (with zero occurring at full extension). Wrenches on the mass center can be applied by the legs – which are assumed to be massless – when in contact with the ground, as well by the spine at the pin joint. For generality we consider these wrenches to be external to the system even when due to compliance⁴.

To reduce the parameter space we make the following assumptions: the front and rear body segments possess identical parameters, each body segment’s mass center is located at the leg hip, and the body segments individually possess no moment of inertia. The model can then be parametrized by $\mathbf{p} = (m, d)^T$, where $m \in \mathbb{R}^+$ denotes total mass and $d \in \mathbb{R}^+$ denotes extended body length. The distance between the front and rear masses \bar{d} is given by $\bar{d} = d \cos(\psi/2)$, which we later use as a convenient surrogate for ψ .

¹A supplementary video of these runs are available at <https://youtu.be/giBBQaqbLFc>.

²See [19] for a full description of bounding and other types of gaits used for locomotion.

³While this is the most common class of robotic core actuation models in the literature, alternatives have been proposed such as [10].

⁴The advent of virtual compliance in legged drive-trains [22], [23] complicates considering compliance as part of the natural system dynamics.

The dynamics of the model are represented as

$$M\ddot{\mathbf{q}} + C\dot{\mathbf{q}} + N = \tau,$$

where

$$M(\mathbf{q}) = \text{diag}\{m, m, \frac{md^2}{8}(1+\cos(\psi)), \frac{md^2}{32}(1-\cos(\psi))\}$$

is the diagonal inertial matrix,

$$C(\mathbf{q}, \dot{\mathbf{q}}) = \begin{pmatrix} 0 & 0 & 0 & 0 \\ 0 & 0 & 0 & 0 \\ 0 & 0 & 0 & -\frac{md^2}{8}\sin(\psi)\dot{\phi} \\ 0 & 0 & \frac{md^2}{16}\sin(\psi)\dot{\phi} & \frac{md^2}{64}\sin(\psi)\dot{\psi} \end{pmatrix}$$

gives the Coriolis terms, the effect of gravity is accounted for by

$$N(\mathbf{q}) = \begin{pmatrix} 0 & mg & 0 & 0 \end{pmatrix}^T,$$

and $\tau \in \mathbb{R}^4$ is the sum of the external wrenches on the mass center.

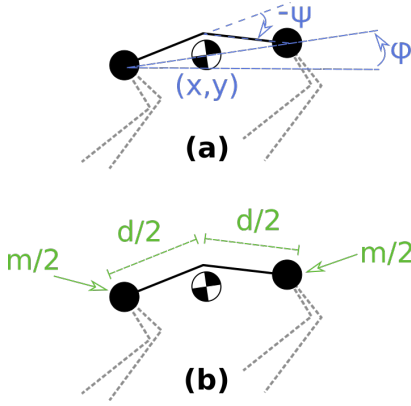


Fig. 1. The reduced-order sagittal-plane spined quadrupedal model consists of two bipedal point masses connected by a massless pin joint. The state of the model shown in (a) is given by $\mathbf{q} = (x, z, \phi, \psi)^T \in \mathcal{Q} = \mathbb{R}^2 \times \mathbb{T}^2$ and its time derivative, where \mathbf{q} respectively consists of the forward and vertical position of the mass center, the body pitch, and the spine angle with respect to full extension. The model is parametrized by the total mass m and extended body length d as shown in (b). The legs are assumed to be massless. The distance between the front and rear masses \bar{d} is given by $\bar{d} = d \cos(\psi/2)$, which we use as a convenient surrogate for ψ .

One potential drawback with this modeling choice is that the inertial matrix loses rank when the spine is fully extended. We avoid numerical issues in simulation with little loss of fidelity by controlling the model to extend the spine just short of this singularity instead of to the fully extended configuration.

III. QUADRUPEDAL PLATFORM

The Inu robot – shown in Figure 2 and introduced in [18] – is composed of two bipedal body segments connected by a parallel elastic-actuated spine. The robot weighs 6.8kg and has a hip-to-hip length of 0.47m at full spine extension.

The spine, a descendant of the design reported in [16], consists of a custom-made fiberglass leaf spring which is actuated in parallel by a belt drive. Vertebrae connect the belt to the fiberglass leaf spring, constraining the spine's bending

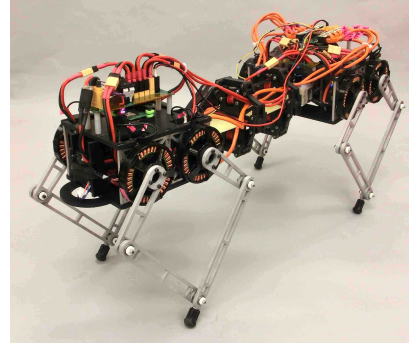


Fig. 2. The Inu robot is composed of two bipedal body segments connected by a parallel elastic-actuated spine. The spine consists of a custom-made fiberglass leaf spring which is actuated in parallel by a belt drive. The belt drive is actuated through a sprocket by two parallel TMotor U8-16 brushless motors housed in the rear body segment. These motors pull on the belt against a fixed sprocket in the front of the robot, allowing the motors to pitch the spine upwards or downwards. Vertebrae connecting the belt drive to the fiberglass leaf spring constrain the bending curvature.

curvature. The belt drive is actuated through a sprocket by two parallel TMotor U8-16 brushless motors⁵ housed in the rear body segment. These motors pull on the belt against a fixed sprocket in the front of the robot, allowing the motors to pitch the spine upwards or downwards. The spine is able to achieve a minimum hip-to-hip distance of 0.27m at maximum bending (20cm less than the hip-to-hip length at full extension), however for this work only moderate spine bending was used. The robot's legs consist of five-bar mechanisms driven by a pair of parallel direct-drive TMotor U8-16 brushless motors adapted from the design reported in [23].

Low-level motor control is done on custom in-house electronics detailed in [24]. An STM32F3⁶ microcontroller housed in the rear body segment is used for high-level control. The only sensors used for control (aside from magnetic encoder readings of motor shafts) are two InvenSense MPU6000⁷ IMUs housed in the front and rear body segments to estimate orientation. Power is provided by a 3-cell lithium polymer battery housed in the front body segment.

IV. EXPERIMENTAL SETUP

A. Bounding Control Strategy

The bounding control strategy used in the experiments builds upon ideas presented in [25] and [26], and is described below only in brief as the focus of this work is the correspondence of the model with the physical robot – saving an in-depth description and analysis of the control scheme for the subject of future work. The control algorithm consists of commanding the front and rear legs to act as modified sagittal-plane Raibert hoppers [25, p. 56] and actuating the spine according to which hopper is in stance. The front and rear body-segment controllers share no state information

⁵<http://www.rctigermotor.com/>

⁶http://www.st.com/content/st_com/en/products/microcontrollers.html

⁷<https://store.invensense.com/>

and are only coupled through the physical dynamics of the body, but this physical coupling is sufficient to give rise to a bounding gait (as described in [26]).

Specifically, the left and right legs of an individual body segment are commanded as one “virtual leg” [25, p. 92] to anchor the Spring Loaded Inverted Pendulum (SLIP) template [27], [28] so as to mimic a radial Hooke’s law spring while in stance. A full description of the virtual compliance control scheme used to achieve the SLIP anchoring is given in [29]. The virtual legs are vertically energized by applying a radial piecewise constant leg force to compress the radial virtual leg spring in the first half of stance and assist its extension in the second half of stance. Forward-speed control is achieved using Raibert’s neutral-point technique [25, p. 40-47] to select a desired leg touchdown angle in flight. The forward speed is further energized by applying a leg torque in stance proportional to the difference between the actual leg angle and the desired liftoff angle of Raibert’s neutral-point controller.

For a bounding gait to emerge (as described in [26]) from the physical coupling between the hopping front and rear body segments, we artificially limit the stance duration of the legs to be 190ms or less, after which the legs are retracted to force the body segment into flight. With longer stance durations, a pronking gait emerges. The causes of this gait bifurcation will be analyzed in future work.

The spine is controlled by commanding a spine retraction to a set angle if the front legs are the only legs in stance, commanding a full spine extension if the rear legs are the only legs in stance, and maintaining the spine’s current angle otherwise.

B. Controller Implementation On-Board the Inu Robot

A stable bounding gait utilizing core actuation was achieved using the above controller on-board the Inu robot. Controller parameters such as the virtual spring stiffness were hand-tuned either on the robot or using the simulation described in Section IV-D to search for a limit cycle. User input at runtime consisted of setting the desired speed via joystick. The only modification made to the algorithm presented in Section IV-A was that the spine extension and retraction were commanded to occur gradually over the course of 100ms because faster retraction and extension resulted in slippage of the spine belt over the driving sprocket.

C. Experiment Design

Two experiments were performed using the robot. In the first (Experiment 1), the robot was documented bounding with spine bending in steady-state at modest speeds so as to examine how well the reduced-order model could be fit to describe the empirical data. In the second (Experiment 2), the robot was recorded bounding at steady-state while keeping its spine rigid – by setting the spine retraction angle in the controller to be equal to the spine extension angle – and then transitioning into a bound utilizing core bending. The purpose of the second experiment is to both demonstrate the stability of the bound over a range of operating points

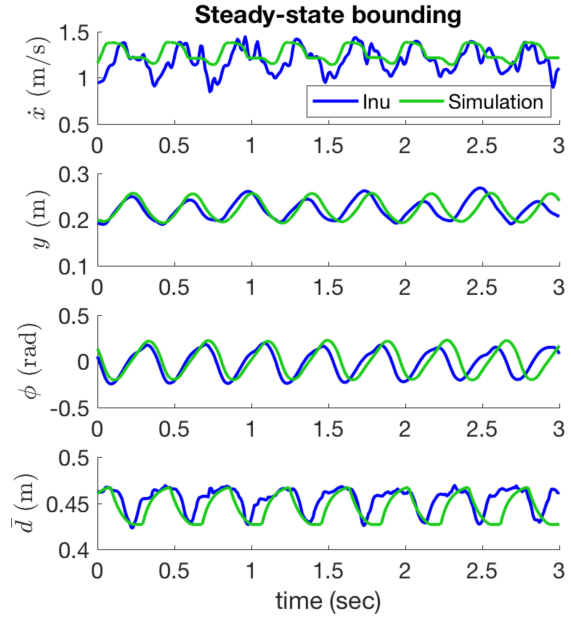
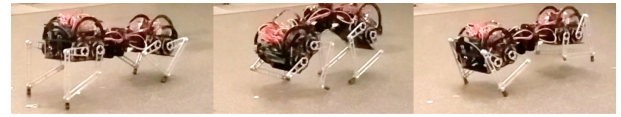


Fig. 3. (Top) Three successive still shots taken of Inu bounding using core actuation. (Bottom) Empirical data of Inu bounding is plotted in blue over the course of 8 strides. Data of the reduced-order model utilizing a nearly identical controller as physically implemented is plotted in green. The data show a close agreement in stride frequency – 2.65Hz for Inu versus 2.58Hz for the simulation – as well as vertical height z and body pitch angle ϕ . The robot decelerates more in mid-stance than in the simulation and the spine bending trajectories are slightly different, the latter likely due to the modification of the spine controller when implemented on the robot to prevent belt slippage as described in Section IV-B.

and evaluate how well the model from Experiment 1 predicts bounding behavior at these different spine-bending operating points.

Kinematic data of the bounding robot was collected using a Qualisys⁸ motion capture system. The kinematic data was fit to the kinematics of the reduced-order model presented in Section II for comparison with the dynamical simulation of the reduced-order model described in Section IV-D.

D. Comparative Bounding Simulation Using the Reduced-Order Model

The reduced-order model presented in Section II was simulated in MATLAB using the controller introduced in Section IV-A for comparison with the robot experimental behaviors described in Section IV-C. Several simplifications were made to reduce the system complexity in simulation with the goal of making future analysis more tractable: linear damping was applied to the simulated legs in the radial and angular directions to account for the physical robot’s motor torque limitations. The spine joint angle was directly actuated using a proportional derivative controller to

⁸<http://www.qualisys.com/>

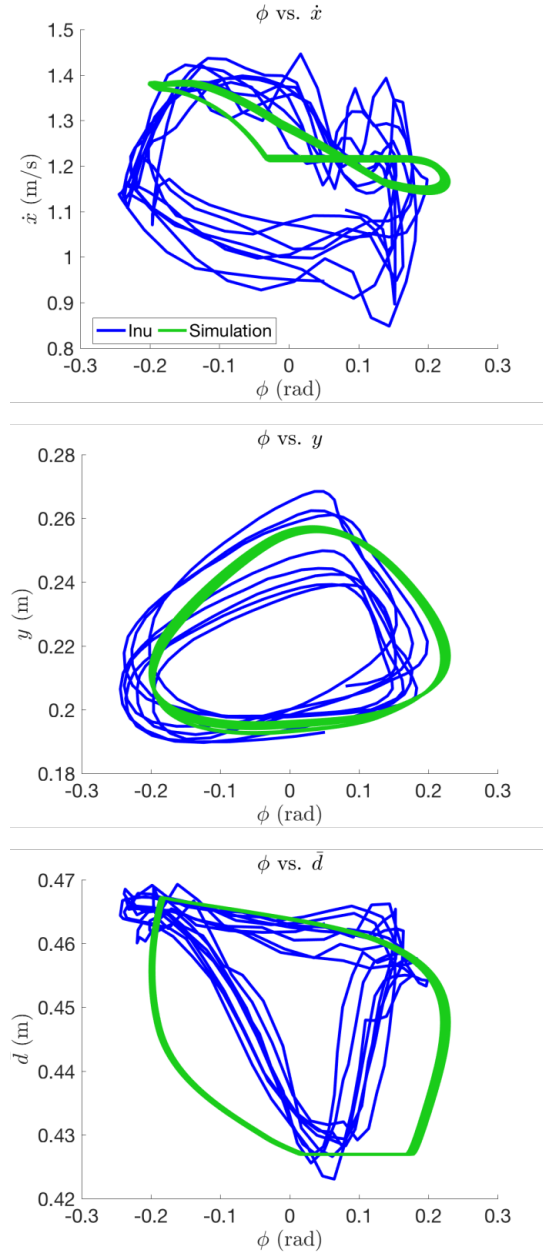


Fig. 4. Projections of the robot state from Figure 3 – bounding in steady-state with core actuation over the course of 8 strides – are plotted in blue. Projections of the simulated robot state utilizing a nearly identical controller are plotted in green. These projections illustrate the close agreement between the robot and simulated model in vertical height z and body pitch angle ϕ (middle). It is unclear what is causing the Inu robot to slow down mid-stride (top) but it is likely due to an unmodeled phenomenon such as energetic losses from leg-ground impacts. The discrepancy in spine trajectory projections (bottom) is expected due to the modification of the spine controller when implemented on the robot to prevent belt slippage as described in Section IV-B.

achieve the desired spine extension, avoiding a complicated characterization of the physical spine mechanism. Aside from these differences, the controller used in simulation was identical to the controller used on the robot.

The four “free” parameters – the leg radial/angular damping and the spine proportional and derivative gains – were used as inputs to hand-tune the simulation to correspond

roughly to the data of Experiment 1 of Section IV-C. This set of parameters was then used to attempt to predict the robot gait transition of Experiment 2 so as to investigate the predictive ability of the controlled model at different desired speeds and spine deflections.

V. EXPERIMENTAL RESULTS

A. Experiment 1: Steady-State Inu Bounding Documentation and Model Correspondence

Steady state bounding was achieved using core actuation on the Inu robot as shown in Figure 3 at a modest average speed of 1.1m/s, or 2.3 body lengths per second and stride frequency of 2.65Hz using a spine retraction distance of $d - \bar{d} = 5\text{cm}$, roughly 10% of the robot’s hip-to-hip length corresponding to a spine angle of $\psi = -0.9$ rad.

The controlled model shows good correspondence with the physical robot. Figure 3 shows that when the fitted model is simulated using a nearly identical controller, it has a stride frequency of 2.58Hz, only a 3% difference. Projections of the state in Figure 4 illustrate a close match in the vertical height and pitching of the model with the robot. The spine trajectories have a different profile, but this is to be expected given the modification of the spine controller when implemented on the robot to prevent belt slippage as described in Section IV-B. The main discrepancy between the simulation and robot is in forward speed. While the simulation forward speed fluctuates only $\pm 0.1\text{m/s}$, the robot forward speed fluctuates $\pm 0.3\text{m/s}$ as the robot slows down significantly in mid-stride. It is unclear what exactly is causing this speed decrease but it is likely due to an unmodeled phenomenon such as energetic losses from leg-ground impacts that could be mitigated with further gait tuning.

B. Experiment 2: Inu Gait Transition and Model Prediction

Inu is documented in Figure 5 successfully transitioning from a rigid-back bound to a core-bending bound while running, demonstrating stability of the control strategy over a range of spine-bending values. The projections of the state during the transition given in Figure 6 suggest a speed benefit conferred by the spine as the average speed increased by 0.4m/s (a 49% increase) when core bending was used. Using core bending also decreased the average pitch angle swept over the course of a stride by 17% and as well as the average vertical height by approximately 3cm.

The results of Figure 7 show that using the model from Experiment 1 to predict bounding performance over the range of operating points in Experiment 2 had only limited success. A slightly larger speed increase was gained by using core actuation than was predicted by the simulation, and the predictions for the other states were relatively poor. These discrepancies show that while the model appears to be descriptive enough to capture the limit cycle behavior shown in Figure 4, we are not yet able to use it predictively over a range of operating points.

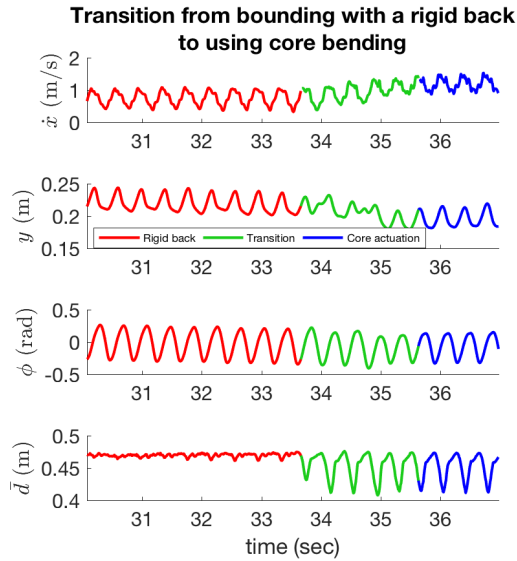


Fig. 5. Documentation of the Inu robot transitioning from a bound with a rigid-back to a bound using core bending. The rigid-back bound was achieved by commanding the spine controller to prevent core bending, and the bound using core-bending was achieved using the controller described in Sections IV-A and IV-B. Engaging the core increased speed, decreased vertical height, and decreased the average pitch angle swept – as is more clearly illustrated in Figure 6. This data is used in Figure 7 to evaluate the predictive ability of the model.

VI. CONCLUSIONS AND FUTURE WORK

We documented the stable bounding performance using core actuation of the Inu quadrupedal robot and proposed a reduced-order model of this system to capture the introduction of the actuated core degree of freedom. This model was sufficiently descriptive as to roughly represent the robot’s mass center trajectory during a bounding limit cycle when simulated using a nearly identical controller to that used on the robot, thus making it a potential option for low dimensional representations of core actuation in legged locomotion and motivating a future more formal data-driven analysis along the lines of [20], [21]. Empirical results of a running transition from a bound with a rigid back to a bound with core bending suggest a speed benefit derived from the core actuation, which will be carefully examined in future work. Initial efforts towards using the controlled model predictively in estimating Inu’s transition from a rigid-body bound to a bound using core bending saw only limited success, demonstrating the potential limits of such a simple representation. We expect that such simplicity will prove advantageous in reducing the complexity of analyzing spined machines in future endeavors, as simplified descriptive models of legged morphologies have so often done before. Future work will focus on using this model in the formal analysis of Inu’s bounding controller as well as investigating the model’s utility in describing non-steady-state transitional tasks.

ACKNOWLEDGMENT

This work was supported in part by the National Science Foundation Graduate Research Fellowship under Grant No.

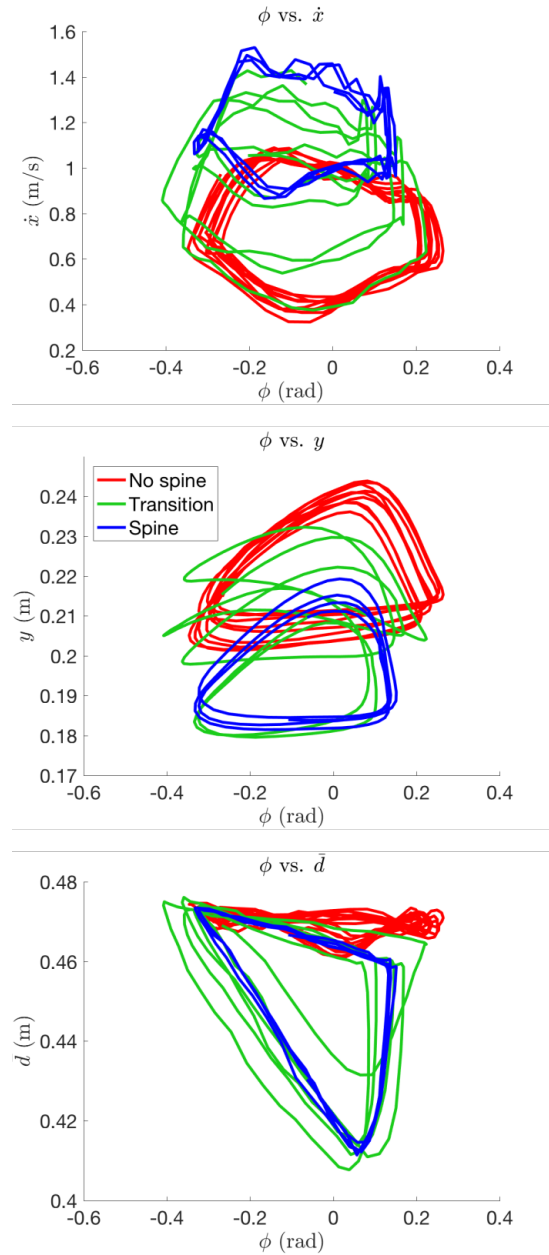


Fig. 6. Projections of the state trajectories shown in Figure 5. When engaging the core, the robot’s average speed increased by 0.4m/s to 49% more than its original speed (top). The average pitch angle swept over the course of a stride decreased by 17% and vertical height decreased by approximately 3cm (middle).

DGE-0822 held by the first author and in part by ONR grant #N00014-16-1-2817, a Vannevar Bush Fellowship sponsored by the Basic Research Office of the Assistant Secretary of Defense for Research and Engineering held by the second author. We thank Benjamin Kramer and Benjamin Bernstein for their support in maintaining and improving the Inu platform.

REFERENCES

- [1] X. Zhou and S. Bi, “A survey of bio-inspired compliant legged robot designs,” *Bioinspiration & biomimetics*, vol. 7, no. 4, p. 041001, 2012.

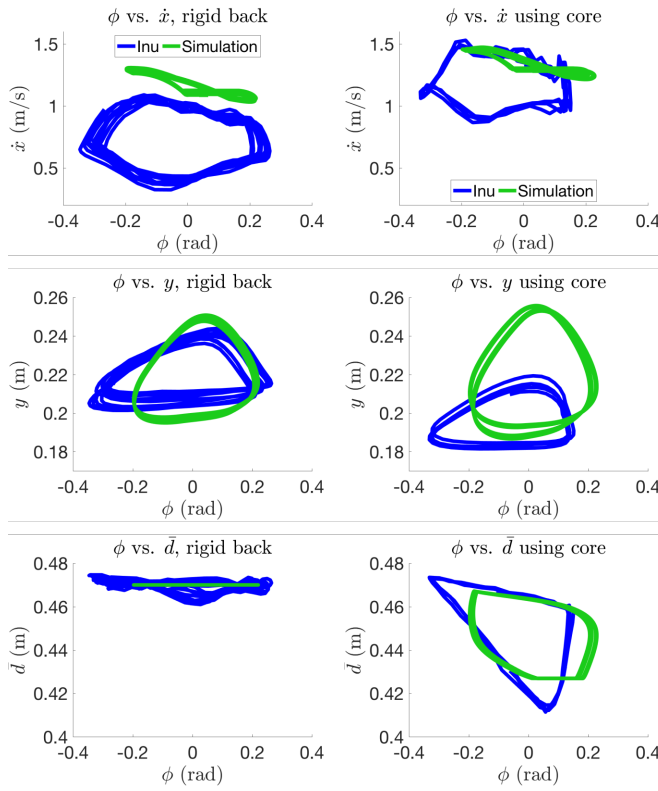


Fig. 7. Model predictions (green) versus empirical data (blue) of the bounding Inu robot transitioning from a bound with a rigid back (left column) to a bound using core bending (right column). A larger speed increase was gained by using core actuation than was predicted by the simulation (top row). The predictions of the vertical height, pitch angle, and spine angle trajectories of the mass center offered by the simulation are relatively poor (middle and bottom rows). These discrepancies show that while the model appears to be descriptive enough to capture the limit cycle behavior shown in Figure 4, we are not yet able to use it predictively over a range of operating points.

[2] M. S. Fischer and H. Witte, "Legs evolved only at the end!" *Philosophical Transactions of the Royal Society A: Mathematical, Physical and Engineering Sciences*, vol. 365, no. 1850, pp. 185–198, 2007.

[3] N. Schilling and R. Hackert, "Sagittal spine movements of small therian mammals during asymmetrical gaits," *Journal of Experimental Biology*, vol. 209, no. 19, pp. 3925–3939, 2006.

[4] N. Schilling and D. R. Carrier, "Function of the epaxial muscles in walking, trotting and galloping dogs: Implications for the evolution of epaxial muscle function in tetrapods," *Journal of Experimental Biology*, vol. 213, no. 9, pp. 1490–1502, 2010.

[5] N. Schilling, "Evolution of the axial system in craniates: Morphology and function of the perivertebral musculature," *Frontiers in Zoology*, vol. 8, 2011.

[6] R. M. Alexander, "Why mammals gallop," *Integrative and Comparative Biology*, vol. 28, no. 1, pp. 237–245, 1988.

[7] R. J. Full and D. E. Koditschek, "Templates and anchors: Neuromechanical hypotheses of legged locomotion on land," *Journal of Experimental Biology*, vol. 202, no. 23, pp. 3325–3332, 1999.

[8] T. Libby, T. Y. Moore, E. Chang-Siu, D. Li, D. J. Cohen, A. Jusufi, and R. J. Full, "Tail-assisted pitch control in lizards, robots and dinosaurs," *Nature*, vol. 481, no. 7380, pp. 181–186, 2012.

[9] T. Libby, A. M. Johnson, E. Chang-Siu, R. J. Full, and D. E. Koditschek, "Comparative design, scaling, and control of appendages for inertial reorientation," *IEEE Transactions on Robotics*, vol. 32, no. 6, pp. 1380–1398, Dec 2016.

[10] Q. Zhao, H. Sumioka, K. Nakajima, X. Yu, and R. Pfeifer, "Spine as an engine: Effect of spine morphology on spine-driven quadruped locomotion," *Advanced Robotics*, vol. 28, no. 6, pp. 367–378, 2014.

[11] S. Pouya, M. Khodabakhsh, A. Sprwitz, and A. Ijspeert, "Spinal joint compliance and actuation in a simulated bounding quadruped robot," *Autonomous Robots*, pp. 1–16, 2016, article in press.

[12] U. Culha and U. Saranlı, "Quadrupedal bounding with an actuated spinal joint," in *Proceedings - IEEE International Conference on Robotics and Automation*, 2011, pp. 1392–1397.

[13] Q. Cao and I. Poulakakis, "Quadrupedal bounding with a segmented flexible torso: Passive stability and feedback control," *Bioinspiration and Biomimetics*, vol. 8, no. 4, 2013.

[14] M. Khoramshahi, A. Sprowitz, A. Tuleu, M. N. Ahmadabadi, and A. J. Ijspeert, "Benefits of an active spine supported bounding locomotion with a small compliant quadruped robot," in *Proceedings - IEEE International Conference on Robotics and Automation*, 2013, pp. 3329–3334.

[15] G. A. Folkertsma, S. Kim, and S. Stramigioli, "Parallel stiffness in a bounding quadruped with flexible spine," in *IEEE International Conference on Intelligent Robots and Systems*, 2012, pp. 2210–2215.

[16] J. L. Pusey, J. M. Duperret, G. C. Haynes, R. Knopf, and D. E. Koditschek, "Free-standing leaping experiments with a power-autonomous elastic-spined quadruped," in *SPIE Defense, Security, and Sensing*, vol. 8741. International Society for Optics and Photonics, 2013, pp. 87410W–87410W.

[17] J. M. Duperret, G. D. Kenneally, J. L. Pusey, and D. E. Koditschek, "Towards a comparative measure of legged agility," in *International Symposium on Experimental Robotics*, Marrakech/Essaouira, Morocco, June 2016.

[18] J. Duperret, B. Kramer, and D. E. Koditschek, "Core actuation promotes self-manipulability on a direct-drive quadrupedal robot," in *International Symposium on Experimental Robotics*, October 2016, in press.

[19] A. A. Biewener, *Animal locomotion*. Oxford University Press, 2003.

[20] S. Revzen and M. Kvalheim, "Data driven models of legged locomotion," in *Proceedings of SPIE - The International Society for Optical Engineering*, vol. 9467, 2015.

[21] H. . Maus, S. Revzen, J. Guckenheimer, C. Ludwig, J. Reger, and A. Seyfarth, "Constructing predictive models of human running," *Journal of the Royal Society Interface*, vol. 12, no. 103, 2015.

[22] D. J. Hyun, S. Seok, J. Lee, and S. Kim, "High speed trot-running: Implementation of a hierarchical controller using proprioceptive impedance control on the mit cheetah," *International Journal of Robotics Research*, vol. 33, no. 11, pp. 1417–1445, 2014.

[23] G. Kenneally, A. De, and D. E. Koditschek, "Design principles for a family of direct-drive legged robots," *IEEE Robotics and Automation Letters*, vol. 1, no. 2, pp. 900–907, 2016.

- [24] A. De and D. E. Koditschek, "The Penn Jerboa: A platform for exploring parallel composition of templates," Online: <http://arxiv.org/abs/1502.05347>, http://repository.upenn.edu/ese_reports/16, Tech. Rep., Feb 2015, arXiv:1502.05347.
- [25] M. H. Raibert, *Legged Robots That Balance*. Cambridge: MIT Press, 1986.
- [26] A. De and D. E. Koditschek, "Vertical hopper compositions for reflexive and feedback-stabilized quadrupedal bounding, pacing, pronking and trotting," (*under review*), Dec. 2016.
- [27] R. Blickhan, "The spring-mass model for running and hopping," *Journal of Biomechanics*, vol. 22, no. 11-12, pp. 1217–1227, 1989.
- [28] U. Saranli, W. J. Schwind, and D. E. Koditschek, "Toward the control of a multi-jointed, monopod runner," in *Proceedings of the IEEE International Conference on Robotics and Automation*, vol. 3, 1998, pp. 2676–2682.
- [29] J. M. Duperret and D. E. Koditschek, "An empirical investigation of legged transitional maneuvers leveraging raiberts scissor algorithm," in *2015 IEEE International Conference on Robotics and Biomimetics (ROBIO)*. IEEE, Dec 2015, pp. 2531–2538.